Molecular Neurobiology (2019) 56:336–349
https://doi.org/10.1007/s12035-018-1089-6

Extracellular Galectin-3 Induces Accelerated Oligodendroglial Differentiation Through Changes in Signaling Pathways and Cytoskeleton Dynamics

Laura Thomas[1] · Laura Andrea Pasquini[1]

Received: 4 January 2018 / Accepted: 16 April 2018 / Published online: 27 April 2018

Abstract

Galectin-3 (Gal-3) is a chimeric protein structurally composed of unusual tandem repeats of proline and short glycine-rich segments fused onto a carbohydrate recognition domain. Our studies have previously demonstrated that Gal-3 drives oligodendrocyte (OLG) differentiation to control myelin integrity and function. The cytoskeleton plays a key role in OLG maturation: the initial stage of OLG process extension requires dynamic actin filament assembly, while subsequent myelin wrapping coincides with the upregulation of actin disassembly proteins which are dependent on myelin basic protein (MPB) expression. In this context, the aim of the present work was to elucidate the mechanism by which recombinant Gal-3 (rGal-3) induces OLG maturation, giving special attention to the actin cytoskeleton. Our results show that rGal-3 induced early actin filament assembly accompanied by Erk signaling deactivation, which led to a decrease in the number of platelet-derived growth factor receptor α (PDGFRα)+ cells concomitantly with an increase in the number of 2′,3′-cyclic-nucleotide 3′-phosphodiesterase (CNPase)+ cells at 1 day of treatment (TD1), and Akt signaling activation at TD1 and TD3. Strikingly, rGal-3 induced an accelerated shift from polymerized to depolymerized actin between TD3 and TD5, accompanied by a significant increase in MBP, gelsolin, Rac1, Rac1-GTP, and β-catenin expression at TD5. These results were strongly supported by assays using Erk 1/2 and Akt inhibitors, indicating that both pathways are key to rGal-3-mediated effects. Erk 1/2 inhibition in control-treated cells resembled an rGal-3 like state characterized by an increase in MBP, β-catenin, and gelsolin expression. In contrast, Akt inhibition in rGal-3-treated cells reduced MBP, β-catenin, and gelsolin expression, indicating a blockade of rGal-3 effects. Taken together, these results indicate that rGal-3 accelerates OLG maturation by modulating signaling pathways and protein expression which lead to changes in actin cytoskeleton dynamics.

Keywords Oligodendrocytes · Galectin-3 · actin · gelsolin · Akt

Introduction

In the central nervous system (CNS), oligodendrocytes (OLG) are the cells in charge of producing the myelin sheaths which wrap axons in order to promote saltatory conduction of the nervous impulse and give metabolic support [1]. OLG go through different maturation states defined by cell morphology and the specific expression of lineage markers. After stem cell specification toward the OLG lineage, OL progenitor cells (OPC) present a bipolar morphology, express platelet-derived growth factor receptor α (PDGFRα), and have migratory and proliferative capacity; later, OPC mature into pre-OLG, extending ramifications and expressing markers like 2′,3′-cyclic-nucleotide 3′-phosphodiesterase (CNPase); finally, these pre-OLG become mature OLG, producing myelin proteins such as MBP and generating myelin sheaths which are capable of axon myelination [2, 3].

Highlights Gal-3 drives early OLG process outgrowth by fostering actin cytoskeleton assembly and a decrease in Erk activation.
Gal-3 regulates OLG maturation by inducing Akt activation and MBP expression, which promote gelsolin release and actin cytoskeleton disassembly.

Electronic supplementary material The online version of this article (https://doi.org/10.1007/s12035-018-1089-6) contains supplementary material, which is available to authorized users.

✉ Laura Andrea Pasquini
laupasq@yahoo.com

[1] Department of Biological Chemistry, School of Pharmacy and Biochemistry, Institute of Chemistry and Biological Physicochemistry (IQUIFIB), University of Buenos Aires and National Research Council (CONICET), Junín 956, C1113 Buenos Aires, Argentina

In this process, the actin cytoskeleton is involved in two sequential steps recently described [4–6]: in a first step, OPC extend and generate ramifications thanks to actin polymerization and, when MBP is expressed, OPC trigger axon ensheathing by means of massive cytoskeleton depolymerization. MBP plays a crucial role by binding to phosphatidylinositol 4,5-bisphosphate (PIP2) on OLG plasma membrane, thus displacing proteins that also bind to this inositol [7, 8]. Among these proteins, cofilin and gelsolin depolymerize the cytoskeleton after being displaced from PIP2 [6].

Actin is present in cells in two states: monomeric G-actin which binds ATP or ADP, or a filamentous polymer of G-actin called F-actin, with a positive pole in which G-actin-bound ATP units are added, and a negative pole in which actin binds ADP and depolymerization occurs. F-actin can be organized in different ways to generate different structures such as filopodia, which comprise F-actin beams, and lamellipodia, which consist of network-shaped filaments, among others. As actin polymerization is a thermodynamically unfavorable process, nucleating proteins allow polymerization to be triggered [9]. In lamellipodia, this mechanism is regulated by a protein complex called Arp2/3, crucial in the first step of oligodendroglial maturation [6]. This complex is regulated by proteins of the Wasp/Scar family, within which WAVE1 and WAVE2 are important in OLG [10] and are in turn activated by monomeric GTPases such as Rac1 in lamellipodia. In addition, proteins such as profilin allow the exchange of ADP to ATP for actin monomer reuse, but act as monomer scavengers when overexpressed [11].

The expression of myelin proteins is regulated in part by the activation of signaling cascades, among which Erk1/2, Akt, and β-catenin are important in OLG. Current knowledge on the role of these signaling cascades seems rather controversial: some authors claim that the Erk pathway could allow the passage from OPC to pre-OLG and the Akt pathway from pre-OLG to mature OLG [12, 13], while other authors have reported opposite functions [14, 15]. With regard to the β-catenin pathway, some authors define it as an inhibitor [16–18] and others as a promoter of OLG maturation [19–21].

Galectin-3 (Gal-3) is a carbohydrate-binding protein belonging to the lectin family. It is composed of a carbohydrate recognition domain (CRD) and an N-terminal domain composed of proline and glycine-rich sequences. This latter domain enables Gal-3 to form oligomers in the presence of ligands, allowing the formation of lattices in the plasma membrane and triggering intracellular events [22]. Gal-3 is described mainly as an inflammation-modulating protein, a regulator of apoptosis, a component of the spliceosome complex, a regulator of signaling cascades [23] and, in tumor cells, the activator of Rac1 [24, 25], generating an increase in the turnover of actin filaments, among other functions. In our laboratory we demonstrated the ability of Gal-3 as a promoter of myelin formation [26], a modulator of microglial phenotype, and a promoter of remyelination after demyelination by cuprizone [27, 28]. Other reports have shown that OPC exposed to cerebrospinal fluid from patients with progressive primary multiple sclerosis had an augmented Gal-3 expression and were more ramified than those under control treatment [29].

In this work, we demonstrate that Gal-3 promotes an acceleration of oligodendroglial maturation, generates changes in the activation of Erk1/2, Akt, and β-catenin signaling cascades, and induces the expression of actin-related proteins, accelerating the shift from polymerizating to despolymerizating actin cytoskeleton dynamics. Taken together, these results deepen current knowledge about the role of Gal-3 in oligodendroglial maturation, putting emphasis on the molecular mechanisms involved.

Materials and Methods

Materials

Bovine insulin, progesterone, putrescine, sodium selenite, T3, penicillin, 3-(4,5-dimethylthiazol-2-yl)-2,5-diphenyl tetrazolium bromide (MTT), Hoechst 33342, streptomycin, polymyxin-B-agarose, alpha-lactose-agarose, kanamycin, and phosphatase inhibitor cocktail were obtained from Sigma Aldrich (St. Louis, MO, USA). Fetal bovine serum (FBS) was purchased from CRIPION (Buenos Aires, Argentina). Protease inhibitor cocktail was obtained from Roche Applied Science (Mannheim, Germany). DMEM/F12 and Alexa Fluor 488 tetrafluorophenyl (TFP) ester kit were purchased from Life Technologies (Carlsbad, CA, USA). Recombinant human PDGF-AA was purchased from PeproTech (Veracruz, Mexico). Recombinant human bFGF was a kind gift from Dr. Baldi (IBYME, Buenos Aires, Argentina). Bacteria BL21DE3 star and plasmid pET28b+-Gal-3 were a gift from Guillermo Ramos (School of Biochemistry and Biological Sciences, Santa Fe, Argentina). Anti-MBP was a generous gift from Dr. Anthony Campagnoni (University of California, Los Angeles). Anti-RIP antibody was obtained from Chemicon Int. (Temecula, CA, USA). Anti-PDGFRα was purchased from Neuromics (Edina, MN, USA). Anti-Gal-3 antibody was prepared in F.T.L's laboratory and used as described (Acosta-Rodriguez et al. 2004). Anti-Akt, anti-phosphorylated Akt, anti-Erk 1/2, anti-phosphorylated Erk 1/2, anti-gelsolin, anti-WAVE2, anti-profilin, anti-GAPDH, LY294002, and U0126 were purchased from Cell Signaling Technology (Danvers, MA, USA). Anti-Rac1 was purchased from Millipore (Billerica, MA, USA). Anti-beta-catenin was obtained from Abcam (Cambridge, UK). Sir700-actin kit was obtained from Cytoskeleton Inc. (Denver, CO, USA). Phalloidine Cy3 was a kind gift from Dr. Ana Rodriguez (University of Buenos Aires, Argentina). Secondary antibodies were obtained from Jackson

Immuno Research Co. Laboratories (West Grove, PA, USA). Lactose and sucrose were purchased from Biopack (Buenos Aires, Argentina). All other chemicals used were of analytical grade of the highest available purity.

rGal-3 Production and Purification

rGal-3 was obtained using *Escherichia coli* BL21DE3 "star" transformed with pET 28b+-Gal-3 plasmid based on Salomonsson et al. 2010 [30]. Preculture of bacteria in Terrific broth (TB; yeast extract 24 g/l, tryptone 20 g/l, glycerol 4 ml/l, KH_2PO_4 0.017 M, K_2HPO_4 0.072 M) with 2 mM of glucose and 50 μg/mL kanamycin reached stationary phase within 18–20 h at 37 °C and 200 rpm. Afterwards, the preculture was diluted 1/80 in TB with kanamycin and cultured at 37 °C until 0.8 O.D at 600 nm was reached. Induction with 1 mM IPTG for 3 h was performed at 28 °C and 200 rpm. After induction, bacteria were pelleted and resuspended in Tris buffer with protease inhibitor and sonicated through 14 pulses of 30 s with Branson Sonifier 250, with an output power of 35 W and a duty cycle of 0.5%. An aliquot was plated in TB-agar for colony forming unit (CFU) counting. The remaining material was centrifuged and an aliquot of the supernatant (SN) was tested for hemagglutination and analyzed by western blot to identify the presence of rGal-3. The rGal-3 present in the SN after bacterial lysis and centrifugation was purified from other bacterial proteins by lactose affinity chromatography and from lipopolysaccharide (LPS) by polymyxin B affinity chromatography and an aliquot was analyzed by SDS-PAGE and western blot to identify the presence of rGal-3. Further confirmation of rGal-3 presence and integrity in the eluate was performed by mass spectrometry (Fig. S1).

OLG Cultures

Primary OLG cultures were performed as described by McCarthy and de Vellis (1980). Cerebral hemispheres were dissected out from newborn rats (P0–2), freed of meninges, and dissociated by mechanic disaggregation in DMEM F12 containing 5 mg/ml streptomycin and 5 U/ml penicillin, supplemented with 10% FBS. The cell suspensions were seeded in poly-L-lysine-coated 75-cm^2 tissue culture flasks. After 10 days in culture, microglia were separated by shaking the flask for 1 h in an orbital shaker at 100 rpm/min, and OLG were separated from astrocytes by continuous shaking for 24 h at 150 rpm/min. The cell suspension obtained was filtered through a 15-mm mesh filter and then centrifuged at 300×*g* for 10 min. OLG were grown on poly-L-lysine-coated Petri dishes for western blot studies or on poly-L-lysine-coated coverslips placed in multiwell plates for morphological and immunocytochemical studies or in glass bottom multiwall plates for time lapse studies. OLG purity was more than 95%, as assessed by immunocytochemistry positive cell counting against glial fibrillary acidic protein (GFAP), ionized calcium-binding adapter molecule 1 (Iba1), and oligodendrocyte transcription factor (Olig2), for astrocytes, microglia, and OLG, respectively (data not shown). The purified OLG were maintained in Glia Defined Medium (GDM; DMEM/F12 supplemented with glucose 4 g/l, $NaHCO_3$ 2.4 g/l, insulin 25 mg/l, putrescin 8 mg/l, transferrin 50 mg/l, T3 9.8 mg/l, progesterone 20 nM, sodium selenite 8 mg/l, and biotin 10 mg/l) supplemented with growth factors (PDGFAA 10 ng/ml and bFGF 10 ng/ml) and 0.5% FBS for 48 h. Afterwards, OPC were treated for the times indicated in GDM with 0.5% FBS, without growth factors.

Signaling Pathway Inhibition

OPC were treated with or without LY294002 (10 μM; PI3K inhibitor) or U0126 (10 μM; MEK1, MEK2 inhibitor) for 30 min previous to rGal-3 treatment. Lactose (100 mM; rGal-3 CRD inhibitor) and sacarose (100 mM), the latter as a non-competitive carbohydrate for lactose assays, were incubated with rGal-3 for 30 min before being added to OPC.

Immunocytochemistry

Cells were fixed with 4% PFA for 20 min, rinsed in PBS, permeabilized in 1% Triton X-100 for 30 min (only for cytosolic antigens), and blocked with 5% FCS for 2 h. Incubation with primary antibodies was done overnight at 4 °C. Cells were incubated with a fluorescent-conjugated anti-rabbit, anti-mouse, or anti-goat secondary antibody (Cy3, Alexa Fluor 488 or 649) or with Phalloidin-Cy3 for 90 min. Nuclei were labeled with the fluorescent dye Hoechst 33342 (5 mg/ml 1% DMSO). The preparation was mounted in Mowiol and analyzed by UV light microscopy with an Olympus BX50 microscope (Olympus, Tokyo, Japan) or confocal microscopy. Photographs were taken with a CoolSnap digital camera and ImageJ software was used for image analysis. Confocal images were obtained capturing a stack of images placed at regular intervals through the z axis of an area of interest. Subsequently, a 3D reconstruction was made using the IMARIS 6.3.1 program (BitplaneSci Software). Total PDGFRα, CNPase+ and MBP+ cells per field were counted as antigen-positive cells in 20 randomly selected fields and normalized to Hoechst-positive cells. ImageJ software was also used to quantify reactive or immunoreactive areas and integrated optical density (IOD). Briefly, a threshold was determined for each photograph so that all positive cells were included and the background excluded. The immunoreactive area or IOD for antigen-positive cells was then calculated normalizing the immunoreactive area or IOD to the count of antigen-positive cells. The reactive area or IOD for Phalloidin was normalized to Hoechst-positive nuclei. For soma and ramification IOD and area quantification, a region of interest

(ROI) was determined around the soma of PDGFRα+ cells or around single processes of PDGFRα+ cells. IOD and area were measure out of each ROI.

Real-Time Confocal Microscopy

OPC were plated onto glass bottom multiwell plates coated with poly-L-lysine and cultured in the presence of 0.5% FBS and 10 ng/ml of PDGFAA and bFGF for 48 h. OPC were serum-starved for 3 h, then treated for 1 h with 100nM SiR700 actin to track F-actin. rGal-3 was conjugated to Alexa Fluor 488 using Alexa Fluor 488 TFP ester kit. Real-time confocal microscopy was carried out after 30 min treatment with rGal-3, rGal-3 488, or vehicle. Images were taken every 5 min 18 s at ×20 magnification with Zeiss AxioObserver Z1-LSM710. Z-stacks were reconstructed and analyzed using Fiji software. Random cells were selected out of each condition, and IOD and cell area were measured.

Rac1 Pull-Down Assay

OPC were plated in 60-mm dishes coated with poly-L-lysine and cultured in the presence of 0.5% FBS and 10 ng/ml PDGFAA and 10 ng/ml bFGF for 48 h. OPC were serum-starved for 3 h and then treated with or without rGal-3 for 5 days. Cells were lysed and 500 μg protein was used in a pull-down assay with PAK-PBD beads. The resulting pull-down was then immunoblotted with Rac1 antibody according to the manufacturer's instructions.

Western Blot Analysis

Samples were lysed with RIPA extraction buffer (NaCl 150 mM, EDTA 5 mM, Tris 50 mM, NP-40 1%, SDS 0.1%) supplemented with protease inhibitor cocktail and phosphatase inhibitors cocktail for 5 min on ice. In order to clear debris, lysed OLG were centrifuged for 10 min at 7000 rpm. An aliquot from the SN was used to determine protein concentration using Bradford's method. Equal amounts of protein were separated on SDS-PAGE gels and transferred onto PVDF membranes for western blot analysis. Membranes were incubated with the indicated primary antibodies overnight at 4 °C, followed by incubation with peroxidase-conjugated secondary antibodies. Quantification was conducted using a Gel Pro Analyzer 4.0 system (Gel Pro Analizer Media Cybernetics Gel Pro Analyzer, Bethesda, MD, USA).

Cell Viability

OLG were seeded in 96-well plates coated with poly-L-lysine, at a density of 40,000 cells per well and cultured in the presence of 0.5% FBS and 10 ng/ml of PDGFAA and bFGF for 48 h. Cells were then treated with different concentrations of rGal-3 for 1 day, and later treated with MTT at a final concentration of 0.5 mg/ml for 3 h at 37 °C. A solubilization solution (SDS 10%, HCl 0.01 N) was finally added to each well to dissolve formazan crystals and absorbance was measured at 570 nm (Fig. S2)

Statistical Analysis

Graph-Pad Prism Software was used for data analysis. Results are presented as the mean of at least three independent experiments ± standard error of the mean (SEM). Comparisons were performed using unpaired one-tailed Student's *t* test, one-way analysis of variance (ANOVA), or two-way ANOVA followed by Bonferroni post-hoc tests, where appropriate. A *P* value under 0.05 was considered statistically significant.

Results

We firstly evaluated the changes produced by rGal-3 in OLG differentiation. In the present work, purified rat OLG cultures were maintained in GDM with growth factors (10 ng/ml PDGFAA and 10 ng/ml bFGF) and 0.5% FBS for 48 h and then allowed to differentiate for 5 days in GDM in the absence of growth factors with 0.5% FBS. rGal-3 treatment was initiated 3 h after growth factor withdrawal, which was considered treatment day zero (TD0), and renewed every 48 h (Fig. 1a). As cell viability suffered a statistically significant reduction at rGal-3 concentrations starting at 50 μg/ml, we selected 20 μg/ml as the working concentration (Fig. S2a). Immunocytochemical analyses were used to assess the number of PDGFRα+ OPC, RIP+ immature OLG, and MBP+ mature OLG at TD1, TD3, and TD5, as well as changes in immunoreactive areas and IOD for each marker. Our results show that rGal-3 induced a significant increase in the number of RIP+ cells (Fig. 1c) to the detriment of PDGFRα+ cells (Fig. 1b) at TD1, and a significant increase in MBP+ cells (Fig. 1d) at TD5. In addition, results showed a smaller PDGFRα-reactive area at TD5, a larger RIP-reactive area at TD3, and a larger MBP-reactive area at all three time points in rGal-3-treated cultures regarding controls. Finally, no significant differences were observed in IOD values (Fig. 1a–c, respectively).

As actin assembly is required for OLG process extension, we next tested whether rGal-3 induces early changes in the total area of polymerized actin. To such end, we used F-actin staining with Cy3-phalloidin at 15 and 30 min of treatment. Our results show that rGal-3 induced a significant increase in actin filament at both treatment time points in PDGFRα+ cells (Fig. 2a). This result was strongly supported by real-time confocal microscopy studies of F-actin labeled with Sir700Actin in OPC cultured in the presence or absence of rGal-3 or rGal-3

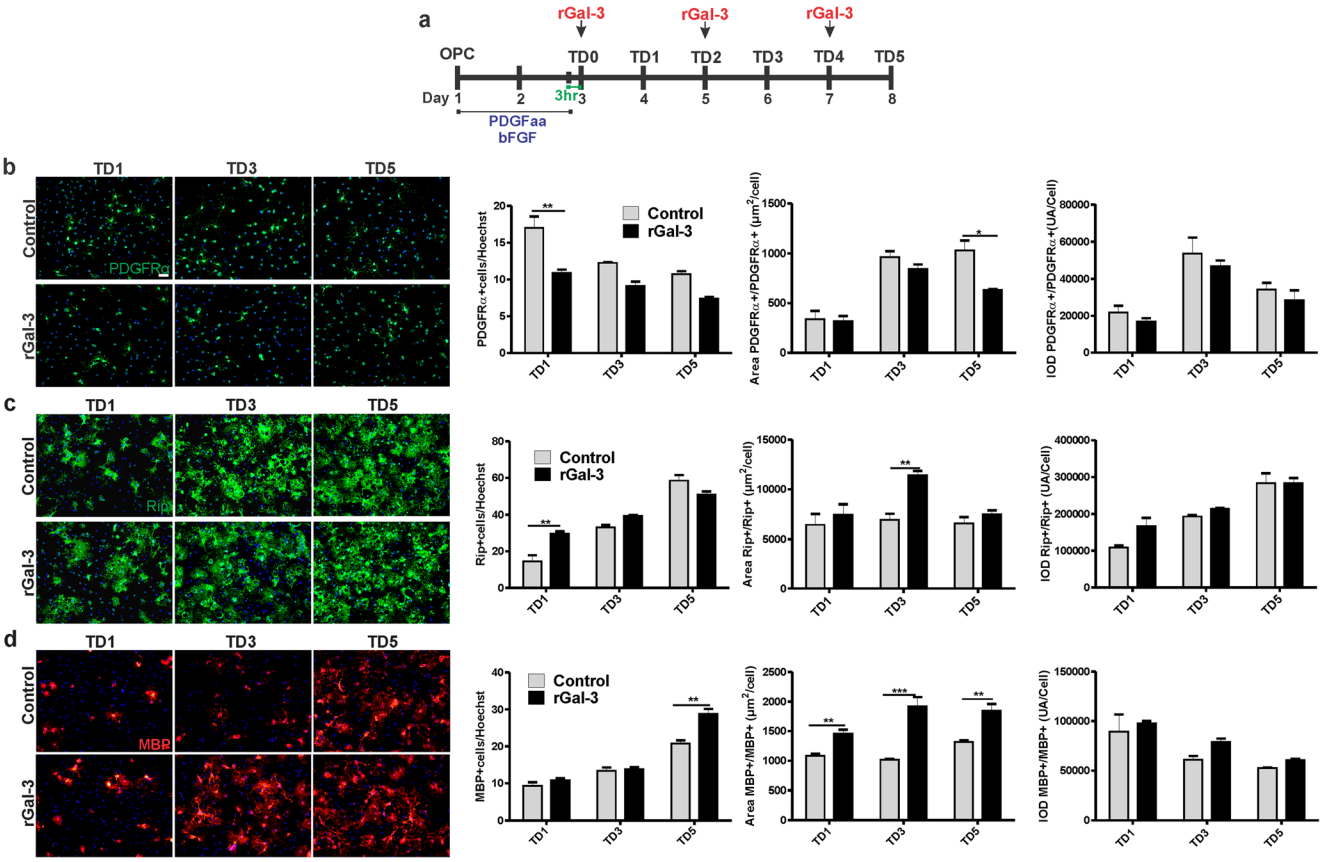

Fig. 1 rGal-3 effect on OLG differentiation. **a** Experimental timeline. For each condition evaluated, cells were fixed and immunostained for: **b** PDGFRα, **c** Rip, and **d** MBP. Graphs show, for every stain performed, immunoreactive cells over number of Hoechst+ nuclei, immunoreactive area over number of immunoreactive cells and IOD over number of immunoreactive cells. All comparisons were performed using two-way ANOVA followed by Bonferroni post hoc test (*$P < 0.05$; **$P < 0.01$; ***$P < 0.001$). Scale bar, 50 μm

488. These studies proved rGal-3 to induce a significant increase in F-actin, which was observed as early as 0.5 h and remained up to the end of treatment (1.6 h). r-Gal-3 488 tracking assays showed Gal-3 to be retained in OPC during the whole experiment (Fig. 2b). In addition, subcellular localization analyses showed significantly higher r-Gal-3-488 reactivity in the soma and bipolar cell ramifications, as compared to multipolar cell ramifications (Fig. 3).

Erk signaling has been implicated in many different aspects of OLG development including proliferation, migration, survival, differentiation, and myelination [31]. Assays were therefore carried out on the early consequences of rGal-3 treatment on Erk signaling, with results showing a significant decrease in the pErk 1/2/tErk 1/2 ratio at 15 and 30 min of treatment (Fig. 4a). In contrast, Erk 1/2 activity was not affected in rGal-3-lactose (Lac)-treated OPC. Given that Lac is a competitive inhibitor for rGal-3 CRD-dependent carbohydrate binding, this finding may indicate that rGal-3 effects are mediated by its CRD (Fig. 4b). Pre-treatment with sucrose (Suc), a non-competitive disaccharide, induced no changes in cell viability or in the effects of rGal-3 treatment (Fig. S2b, c). Taken together, these results indicate that both actin assembly and Erk signaling are early mediators of rGal-3.

Furthermore, we assessed the impact of rGal-3 treatment on different proteins regulating the actin cytoskeleton at longer times: TD1, TD3, and TD5. All times evaluated showed a significant increase in the level of profilin, an actin-binding protein involved in actin cytoskeleton dynamic turnover with a dual compromise. In addition, a significant increase was observed at TD5 in Rac1, a member of the Rho GTPase protein family, without significant changes in WAVE2 (Fig. 5a), a protein receiving upstream signals from Rho GTPase protein family and downstream activating the Arp2/3 complex, which leads to rapid actin polymerization. Moreover, a significant increase in Rac1-GTP, the activated form of Rac1, was induced by rGal-3 treatment at TD5 (Fig. 5b). Strong support for these results was obtained from histological studies showing a significant increase in the F-actin area at TD1 and TD3 and a compensating decrease at TD5 (Fig. 5c). Therefore, rGal-3 induces changes in actin cytoskeleton dynamics and actin-related protein levels which may favor an accelerated OLG maturation.

Next, we evaluated signaling pathways which have been previously described in the control of OLG maturation and myelination [32]. Recent studies suggest that Akt and Erk 1/2 signaling act sequentially to mediate OPC differentiation,

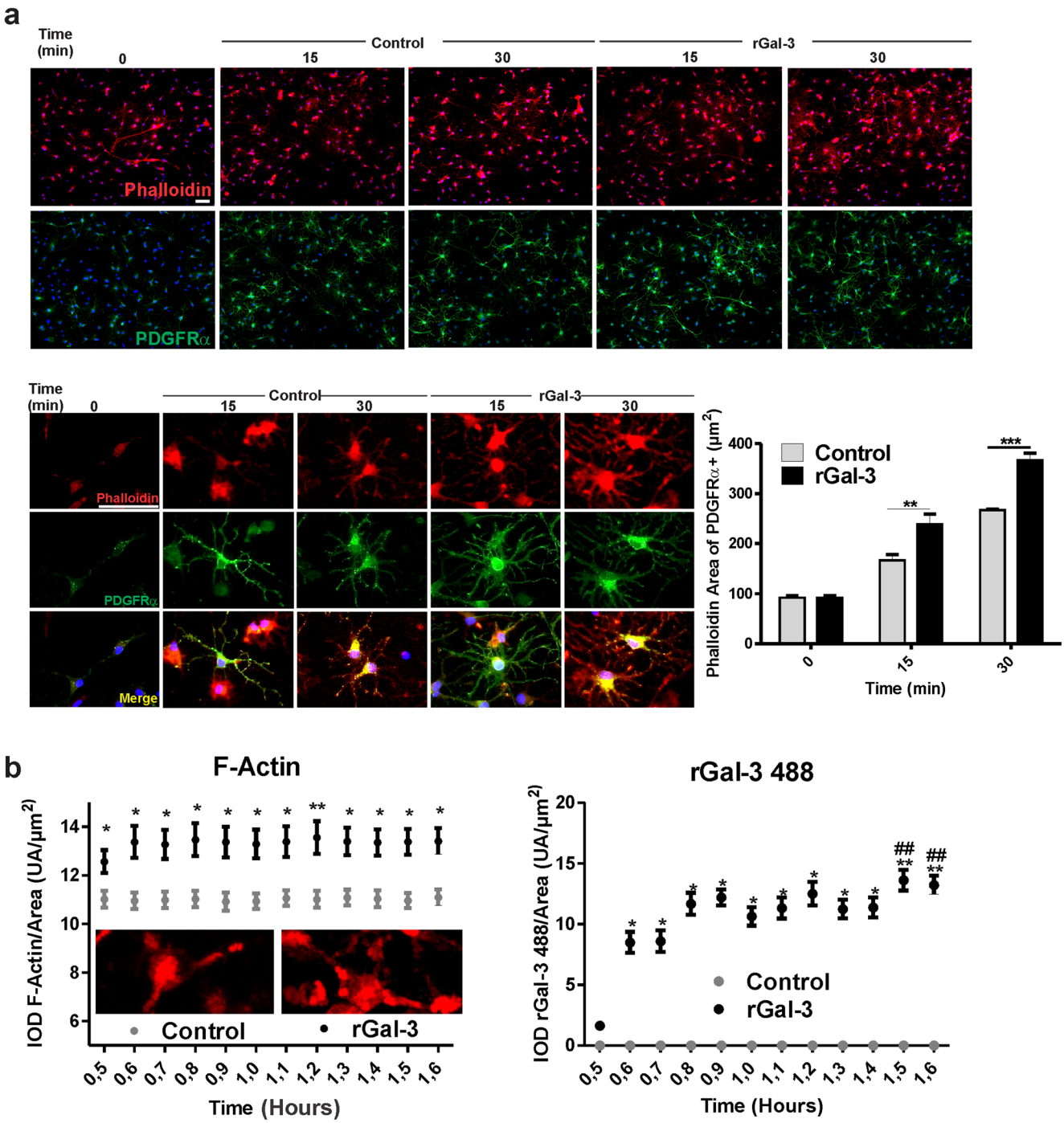

Fig. 2 rGal-3 effect on F-actin after 15 min and 30 min of rGal-3 treatment. **a** OPC were fixed and stained with phalloidin-Cy3 and immunostained for PDGFRα after treatment with or without rGal-3 for the times indicated. A higher magnification panel is included. Graph shows phalloidin area of PDGFRα+ cell quantification. Comparisons were performed using two-way ANOVA followed by Bonferroni post hoc test (**$P < 0.01$; ***$P < 0.001$). **b** OPC were treated with 100 nM Sir700-Actin for 1 h and later treated with or without rGal-3 or rGal-3 488 for the times indicated. Graph shows F-actin IOD per cell area or rGal-3 488 IOD per cell area. Comparisons were performed using two-way ANOVA followed by Bonferroni post hoc test (*$P < 0.05$ **$P < 0.01$; ***$P < 0.001$; * regarding control; # regarding 0.6 and 0.7 h). Scale bar, 50 μm

with Erk 1/2 mediating the transition of early OPC to immature OLG, and Akt/mTOR regulating the process from immature to mature OLG [12]. Our results show that rGal-3 produced a significant increase in the pAkt/tAkt ratio at TD1 and TD3, concomitant with a significant decrease in the pErk 1/2/tErk 1/2 ratio at all times evaluated. Using PI3K inhibitor LY294002 (LY), Akt activation in both control and rGal-3-treated cells was significantly diminished at TD1 and TD3,

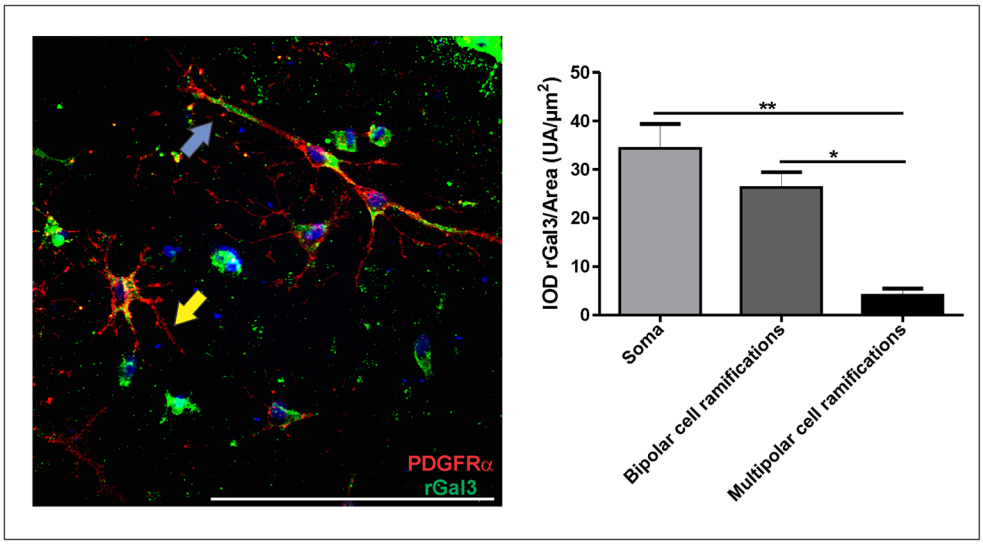

Fig. 3 rGal-3 location in OPC. OPC were fixed and stained with phalloidin-Cy3 and immunostained for PDGFRα after treatment with or without rGal-3 for 30 min. Blue arrow indicates OPC ramification from a bipolar PDGFRα+ cell and yellow arrow indicates OPC ramification from a multipolar PDGFRα+ cell. Graph shows rGal-3 IOD from bipolar and multipolar PDGFRα+ cell soma and ramifications normalized to the area analyzed for each condition. Comparisons were performed using two-way ANOVA followed by Bonferroni post hoc test (*$P < 0.05$; **$P < 0.01$). Scale bar, 50 µm

with a compensatory Erk 1/2 activation in rGal-3-LY-treated cells at all times assayed. Using U0126 (UO), MEK1 and MEK2 inhibitor, we observed Erk 1/2 activation was diminished at all times evaluated in both control and rGal-3-treated cells and partial Akt activation in control cells at TD3 and TD5 and in rGal-3 at TD5. Furthermore, Akt activation was almost completely abolished in rGal-3-Lac-treated cells at all times evaluated, while Erk 1/2 activation was surprisingly not

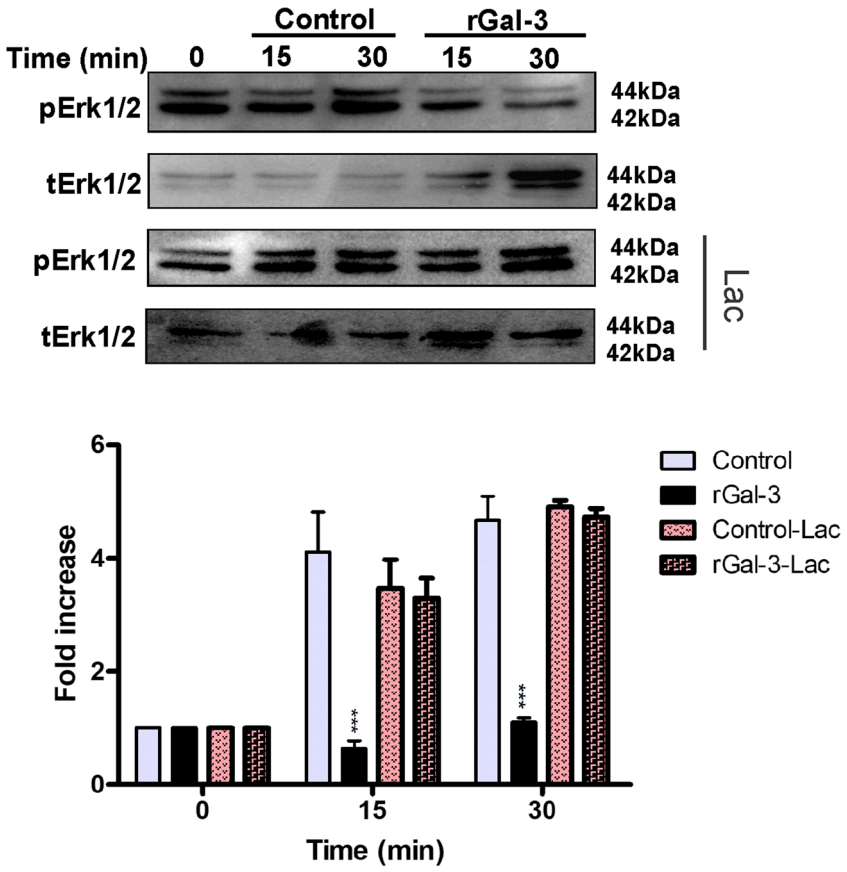

Fig. 4 rGal-3 effect on Erk1/2 phosphorylation after 15 and 30 min of rGal-3 treatment. Representative immunoblot for pErk1/2, total Erk1/2 of OPC treated with or without rGal-3 and with or without lactose for the times indicated. Graph shows immunoblot quantification as fold increases of pErk1/2/tErk1/2 band intensity ratio over Time 0. Comparisons were performed using two-way ANOVA followed by Bonferroni post hoc test (***$P < 0.001$)

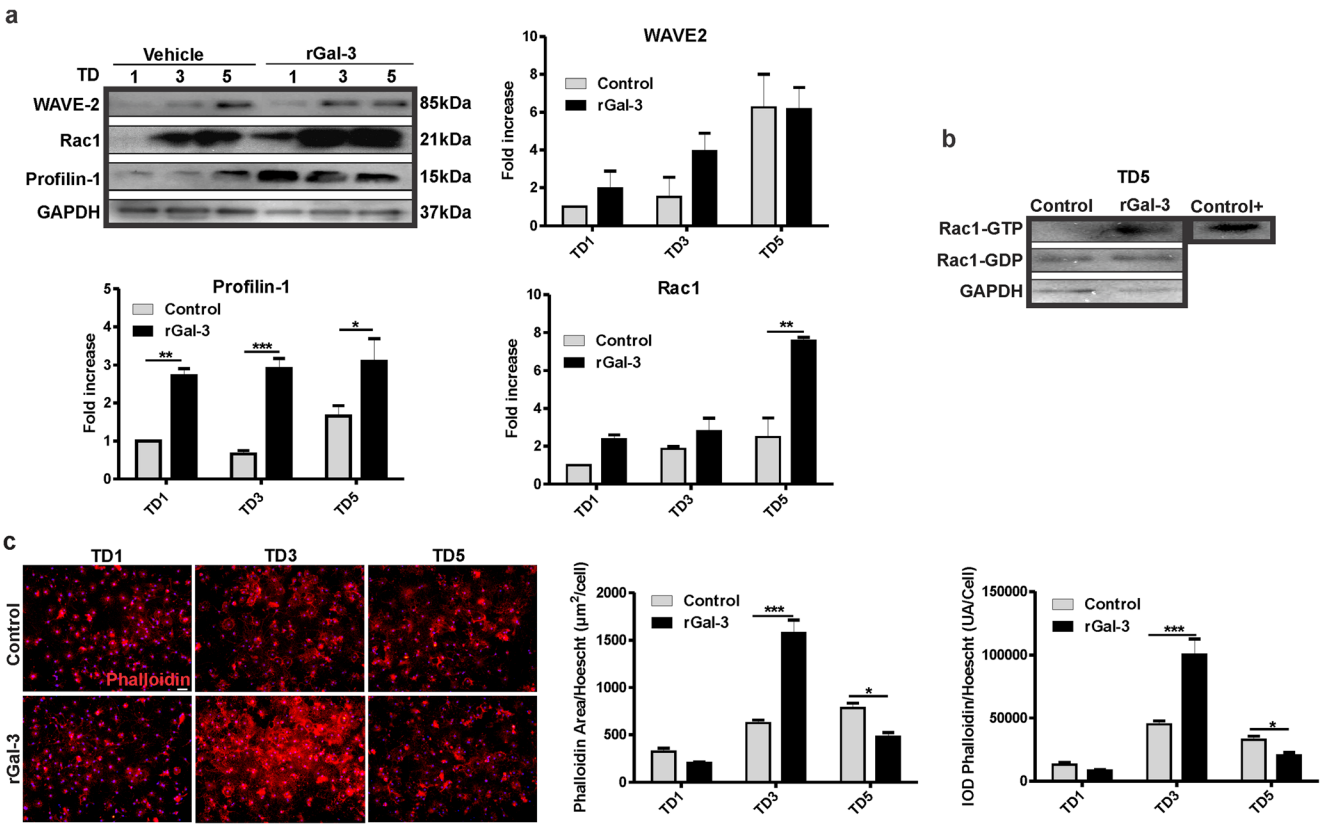

Fig. 5 Effect of rGal-3 on F-actin and on the expression of actin-related proteins. **a** Representative immunoblot and quantification for WAVE-2, Rac1, and profilin-1 band intensities normalized to GAPDH as fold increases over TD1 control. **b** TD5 OLG submitted to Rac1 pull-down assay and immunoblot. Representative immunoblot for Rac1-GTP, Rac1-GDP, and GAPDH. **c** OLG were fixed and stained with phalloidin-Cy3 after treatment of OPC with or without rGal-3 for the times indicated, with treatment renewal every 2 days. Graphs show phalloidin area and IOD normalized to Hoechst+ nuclei. Comparisons were performed using two-way ANOVA followed by Bonferroni post hoc test (*$P < 0.05$; **$P < 0.01$; ***$P < 0.001$). Scale bar, 50 μm

affected, indicating that rGal-3-mediated Akt activation depends on its carbohydrate binding capacity, while Erk 1/2 deactivation depends on protein-protein interactions (Fig. 6a).

On the other hand, the role of Wnt/β-catenin signaling has varying effects on cells of the OLG lineage depending on their developmental stage [33]. Our results revealed that rGal-3 treatment induced a significant increase in the level of β-catenin at TD5 (Fig. 6b). When Akt activation was inhibited by LY, β-catenin levels decreased in both control-LY and rGal-3-LY-treated cells at TD5, indicating that rGal-3 effect on β-catenin depends on Akt activation. Upon inhibition of Erk 1/2 with UO, control cells presented an augmented β-catenin level at TD5 similar to rGal-3-treated cells, while rGal-3- UO-treated cells remained unchanged, indicating that Erk 1/2 inhibition favors an increase in β-catenin. Also, treatment with rGal-3-Lac led to a decrease in β-catenin level compared to control treatment at TD5, which suggests that rGal-3 depends on its CRD to promote this effect.

Next, we assessed MBP and gelsolin expression using Western blot analysis (Fig. 7). In rGal-3-treated OLG, we observed augmented MBP expression at TD5, confirming our immunocytochemical results, accompanied by increased expression of gelsolin, an actin depolymerizing protein. Treatment with LY in both control and rGal-3-treated OLG showed a significant reduction in MBP and gelsolin expression at all times evaluated, indicating that both rGal-3 effects are mediated by Akt. MBP expression was partially increased related to control cells at TD5 in control-UO-treated cells but unaffected in rGal-3-UO-treated cells. Regarding gelsolin, control-UO-treated cells significantly increased expression at the level of rGal-3 and rGal-3-UO-treated cells at all times evaluated. Taken together, these findings indicate that Erk 1/2 inhibition leads to an increase in gelsolin expression and a partial increase in MBP expression. Treatment with Lac and rGal-3 partially reduced MBP expression as compared to rGal-3-treated cells, which again indicates that rGal-3 effects are partly mediated by rGal-3 CRD. This treatment also rendered a reduction in gelsolin expression when compared to rGal-3-treated cells at all times evaluated, which also hints at rGal-3 CRD-mediated effects. No significant changes were induced by Suc, nor was viability affected by any inhibitor (Fig S2 b).

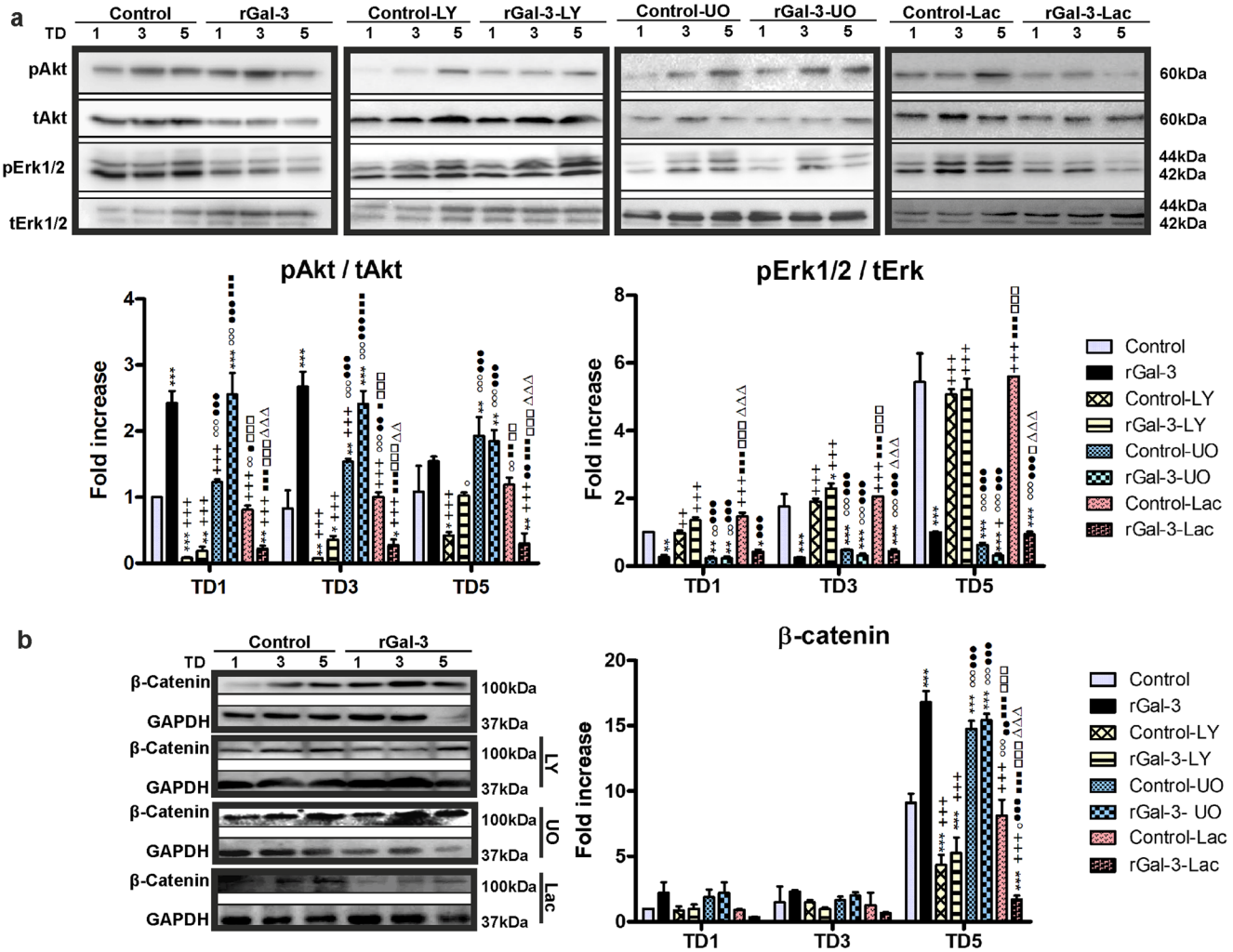

Fig. 6 Effect of rGal-3 on the activation of Akt and Erk1/2. **a** Representative immunoblot for pAkt, tAkt, pErk1/2, and tErk1/2 of TD1, TD3, and TD5 OLG treated with or without rGal-3, LY, UO, or Lac for the times indicated. Graphs show immunoblot quantification for pErk1/2 and pAkt band intensities normalized to tAkt or tErk1/2, respectively, as fold increases over TD1 control. Comparisons were performed using two-way ANOVA followed by Bonferroni post hoc test (*$P < 0.05$; **$P < 0.01$; ***$P < 0.001$; asterisk regarding control; plus sign regarding rGal-3; empty circle regarding control-LY; filled circle regarding rGal-3-LY; filled square regarding control-UO; empty square regarding rGal-3-UO; empty triangle regarding control-Lac)

Discussion

Our results demonstrate that extracellular rGal-3 produces an acceleration of OLG maturation in primary rat OLG cultures, as evidenced by an early increase in the number of CNPase+ cells concomitant with a diminished number of PDGFRα+, and an augmented area and number of MBP+ cells relative to controls. This accelerated Gal-3-induced OLG differentiation was also accompanied by early actin polymerization, as an increase was observed in F-actin area at TD3 followed by a decrease at TD5. These results were coincident with an increased expression of actin-related proteins, in particular, capping protein gelsolin, ADT-ATP exchanger profilin-1, and small GTPase Rac1. Also, rGal-3 altered signaling pathways important to OLG maturation: increased activation of Akt was observed at TD3 and TD5, which was followed by augmented β-catenin protein levels at TD5 and accompanied at all times evaluated by a decrease in activated Erk 1/2. These findings where endorsed by the use of signaling pathway inhibitors and rGal-3 CRD competitive inhibitor lactose (Fig. 8).

At short treatment times, we observed an augmented F-actin area in rGal-3-treated PDGFRα+ cells concomitant with a decrease in phosphorylated Erk1/2. In contrast, in control treatment, phosphorylated Erk1/2 progressively increased, in agreement with the proliferative effect described for this signaling pathway in OLG [34, 35]. This effect was also observed at longer treatment times accounting for OLG programmed maturation and survival [31]. rGal-3-induced Erk1/2 turn-off was sustained at all times evaluated, in line with previously published data showing that rGal-3 deactivates Erk1/2 in retinal pigment cells [36]. rGal-3 effect depended on its CRD binding capacity at short treatment

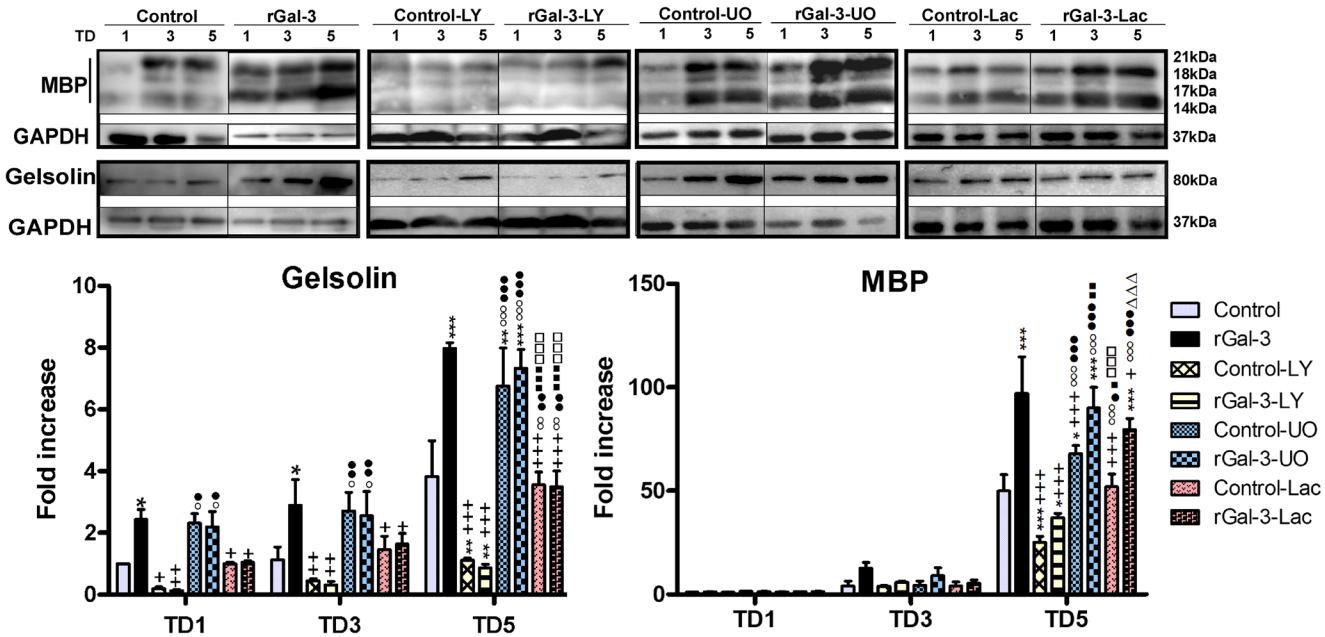

Fig. 7 Effect of rGal-3 on MBP and gelsolin expression. Representative immunoblot for MBP and gelsolin of TD1, TD3, and TD5 OLG treated with or without rGal-3, LY, UO, or Lac for the times indicated. Graphs show immunoblot quantification for MBP or gelsolin band intensities normalized to GAPDH as fold increases over TD1 control. Comparisons were performed using two-way ANOVA followed by Bonferroni post hoc test (*$P < 0.05$; **$P < 0.01$; ***$P < 0.001$; asterisk regarding control; plus sign regarding rGal-3; empty circle regarding control-LY; filled circle regarding rGal-3-LY; filled square regarding control-UO; empty square regarding rGal-3-UO; empty triangle regarding control-Lac)

times but not at longer ones. This may account for rGal-3 binding to glycossacharides in OPC but not in OLG, in concordance with our previous results [26]. Current knowledge demonstrates that this signaling pathway is involved in Arp 2/3 activation as it phosphorylates the WAVE2 regulatory complex, which functions as an Arp 2/3 activator in lamellipodia

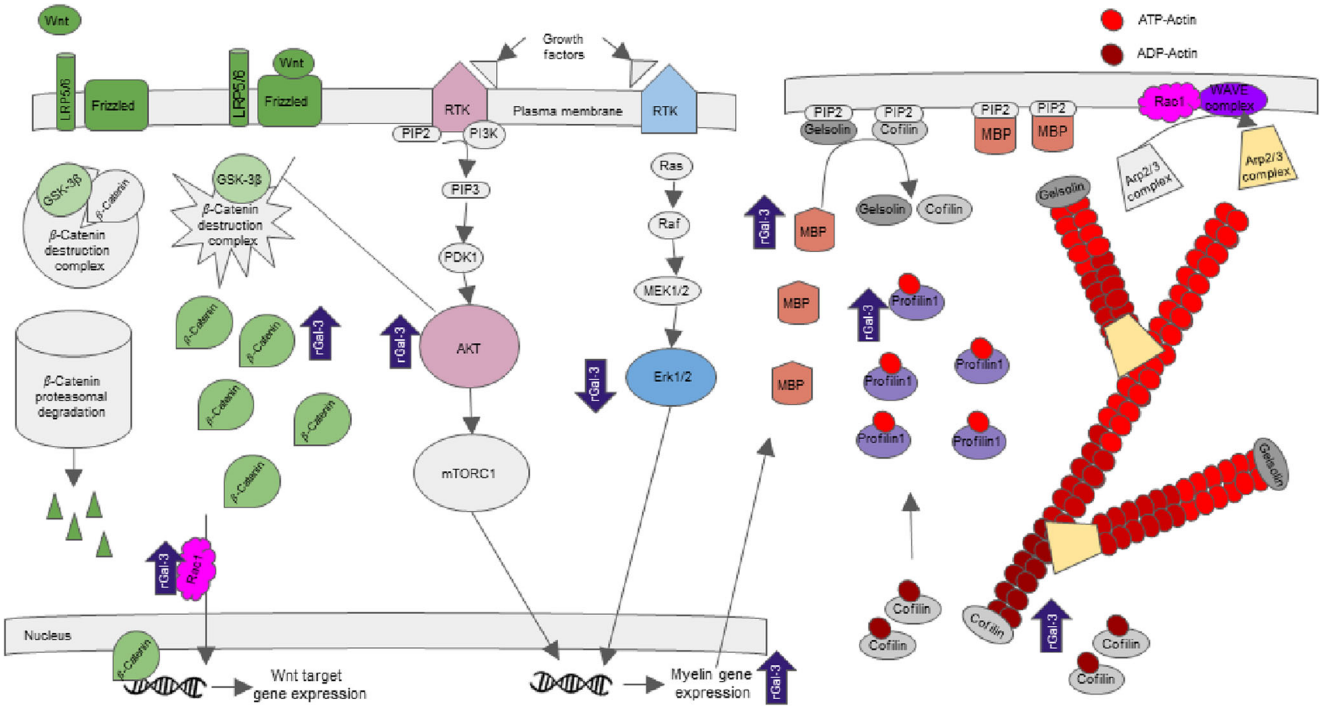

Fig. 8 Graphical abstract. Schematic representation of Wnt/β-catenin (green), AKT/mTOR (pink), Erk/MAPK (blue) signaling networks (left), and cytoskeleton signaling pathway (right) which are important for OLG development and myelination. Extracellular ligands are shown binding to their respective receptors to activate downstream signaling pathways. Black arrows indicate positive interactions and bars indicate inhibitory interactions. Violet arrows indicate where rGal-3 is proposed to influence the above mentioned signaling pathways

at the cell leading edge driving actin polymerization [37]. In addition, the overexpression of actin capping protein gelsolin deactivates Erk1/2 in Jurkat T cells [38]. All these results weave a complex network between rGal-3, Erk 1/2, gelsolin, and actin cytoskeleton, although further work needs to be done in order to elucidate the regulation and consequences of this proposed network.

Previous work by our group has demonstrated a permissive glycophenotype for rGal-3 binding only in OPC [26]. In agreement with this previous finding and further characterizing the effects of rGal-3, the current work shows rGal-3 to bind to bipolar progenitor cells on the soma and ramifications, but to multipolar progenitors only on the soma. Although still PDGFRα+ OPC from a molecular point of view, these multipolar cells showing a higher degree of branching are morphologically more mature than bipolar ones, which hints at rGal-3 preference for less differentiated OPC and limits the temporal window for its action. This may explain why rGal-3 effect on actin dynamics does not seem stable over time. In the current work, we observed pro-polymerization dynamics up to TD3, followed by drastic depolymerization at TD5 which is hand in hand with an increase in gelsolin and MBP expression. These results are in agreement with those reported by Zuchero et al. in 2015 [6], work in which two stages of actin dynamics were described, a polymerization stage until MBP is expressed in large quantities, which then allows the displacement and activation of actin depolymerizing proteins from PIP2. By the use of LY and UO, we observed that MBP and gelsolin are completely dependent on Akt activation and partially on rGal-3 CRD. When OLG were treated with UO, we observed an increase in MBP and gelsolin in control treatment cells, indicating that Erk 1/2 inhibition is important for OLG maturation. These effects may also be due to a slightly compensatory Akt activation in control-UO-treated cells.

In addition, the results reported here on β-catenin could contribute to elucidating the highly controversial role of this signaling pathway in the late stages of OLG differentiation. At TD5, we observed an increase in β-catenin protein levels and in the expression and activation of Rac-1. According to previous reports, Rac1-GTP may aid the translocation of β-catenin to the nucleus, where it fulfills its function as a gene transcription factor [39, 40]. Also, the expression and activation of Rac1 are known to increase with oligodendroglial differentiation leading to correct myelination, which is supported by studies showing more myelin outfoldings in Rac1-KO mice than in control mice [41]. Therefore, the increase in active Rac1 in our system could play a crucial role by allowing the passage of β-catenin to the nucleus, favoring myelin formation. The function of β-catenin in this particular moment in OLG maturation still remains to be determined, as well as the myelin genes transcribed as a consequence. β-catenin was proved to be dependent on Akt activation, rGal-3 CRD, and Erk 1/2 inhibition, indicating a high level of crosstalk among the signaling pathways analyzed.

The role of Akt is of great importance in the maturation of OLG and in the myelination process. For instance, the overexpression of active Akt has been shown to lead to a hypermyelinating phenotype [13, 42], a result also obtained using a conditional KO for PTEN, a phosphatase that directly inhibits Akt [43, 44]. On the other hand, this hypermyelination is reversed when mTOR, an Akt substrate, is inhibited with rapamycin [13]. mTOR is crucial for OLG maturation, as it has been shown to regulate the expression of myelin genes, in particular MBP and PLP, and of proteins related to cholesterol and lipid synthesis [45]. In line with this evidence, our results further show a significant rGal-3-induced increase in the p-Akt/Akt ratio at TD1 and TD3, which could, through mTOR signaling, trigger the increase in MBP expression observed at TD5.

In addition, a relationship has been widely described between the Akt and β-catenin pathways. Akt inhibits GSK-3β, a component of the β-catenin degradation complex [46], so that β-catenin is only slightly phosphorylated and stabilized in the cytoplasm rather than degraded in the proteasome. In 2009, Song et al. reported that Gal-3 promotes the phosphorylation of GSK-3β via Akt signaling in colon cancer cells [47], in line with our observation that β-catenin is augmented at TD5 concomitantly with Akt activation and with the diminished β-catenin levels following Akt inhibition.

Our results also show an increase in the expression of profilin-1 at all times evaluated. This molecule has a dual role, acting as an ADP-ATP exchanger in the actin monomers or as a monomer scavenger according to its level of expression [11]. Furthermore, in fibroblasts, profilin-1 acts as an inhibitor of the Arp 2/3 complex and, consequently, of the formation of lamellipodia [48]. In contrast, in the peripheral nervous system, profilin-1 is described as a crucial molecule for lamellipodia formation and myelination, as these processes are affected in CNP-Cre profilin-1fl/fl mice [49]. To our knowledge, the role of profilin-1 had never been described in OLG before, which is why these results are of great importance and open the door to future research.

In summary, by the use of signaling pathway inhibitors, we partially elucidated the mechanisms by which rGal-3 drives an accelerated OLG maturation. The use of LY, a PI3K inhibitor, reduced β-catenin level and MBP and gelsolin expression, with a compensatory Erk 1/2 activation as previously described [50], in rGal-3-LY-treated OLG, indicating that this pathway is crucial for rGal-3 action. Upon treatment with UO, MEK1 and MEK2 inhibitor, control-UO-treated cells presented an augmented β-catenin level and MBP and gelsolin expression with a slightly compensatory Akt activation, generating a state similar to that of rGal-3-treated OLG. These results lead to the conclusion that Erk 1/2 inhibition is key for OLG maturation. Also, using Lac, a CRD competitive

binding disaccharide, we observed that rGal-3-Erk 1/2 deactivation is only affected in rGal-3-Lac-treated cells at short treatment times, indicating that rGal-3 depends on its CRD and the glycossacharide repertoire present at the time points analyzed. This CRD-dependent effect was also observed with Akt activation, β-catenin, and gelsolin. However, only a mild effect was observed with MBP, indicating that MBP expression is partially driven by rGal-3 CRD and partially by its protein-protein interactions.

It is worth highlighting that our rGal-3 treatment was conducted in a pro-differentiation medium, and that different results could have been obtained in a proliferation medium in the presence of growth factors such as PDGFAA and bFGF. As different from our previous work consisting of a single Gal-3 treatment on OPC during 48–72 h [26], the present study was carried out using rGal-3 renewal every 48 h and OLG evaluation up to TD5, so differences could in fact be the consequence of the different extracellular interactions of rGal-3 with the distinct glycan patterns expressed during OLG differentiation.

In the CNS, extracellular signals are regarded as a communication method between cells, promoting or inhibiting OLG differentiation and (re)myelination [33]. Our previous work has shown that Gal-3 is expressed in microglial cells during myelination and the beginning of remyelination, which favors the induction of an M2 microglial phenotype and OLG differentiation [26–28]. In the present work, we demonstrate that rGal-3 drives early OLG process outgrowth and branching through enhanced actin assembly and a decrease in Erk 1/2 activation, and also regulates OLG maturation by inducing Akt activation and an increase in MBP expression, promoting gelsolin release and actin cytoskeleton disassembly. Taken together, our results postulate rGal-3 as a novel extracellular cue promoting an accelerated OLG maturation.

Acknowledgements We thank Leandro N. Marziali and Teresa Elola for their assistance in rGal-3 production and purification; and to Victoria S.B. Wies Mancini for her help in primary OLG cultures. This study was supported by grants from the Argentine Agency for Promotion of Science and Technology (PICT 2012-0282; PICT 2014-3116), and the University of Buenos Aires (UBACYT-20020130100305BA).

Compliance with Ethical Standards

Conflict of Interest The authors declare that they have no competing financial interest.

References

1. Bercury KK, Macklin WB (2015) Dynamics and mechanisms of CNS myelination. Dev Cell 32:447–458. https://doi.org/10.1016/j.devcel.2015.01.016
2. Nave KA, Werner HB (2014) Myelination of the nervous system: mechanisms and functions. Annu Rev Cell Dev Biol 30:503–533. https://doi.org/10.1146/annurev-cellbio-100913-013101
3. Snaidero N, Simons M (2017) The logistics of myelin biogenesis in the central nervous system. Glia 65:1021–1031. https://doi.org/10.1002/glia.23116
4. Shao Z, Lee X, Huang G, Sheng G, Henderson CE, Louvard D, Sohn J, Pepinsky B et al (2017) LINGO-1 regulates oligodendrocyte differentiation through the cytoplasmic gelsolin signaling pathway. J. Neurosci 37(12):3127–3137. https://doi.org/10.1523/JNEUROSCI.3722-16.2017
5. Nawaz S, Sánchez P, Schmitt S, Snaidero N, Mitkovski M, Velte C, Brückner BR, Alexopoulos I et al (2015) Actin filament turnover drives leading edge growth during myelin sheath formation in the central nervous system. Dev Cell 34:139–151. https://doi.org/10.1016/j.devcel.2015.05.013
6. Zuchero JB, Fu MM, Sloan SA, Ibrahim A, Olson A, Zaremba A, Dugas JC, Wienbar S et al (2015) CNS myelin wrapping is driven by actin disassembly. Dev Cell 34:152–167. https://doi.org/10.1016/j.devcel.2015.06.011
7. Nawaz S, Kippert A, Saab AS, Werner HB, Lang T, Nave KA, Simons M (2009) Phosphatidylinositol 4,5-bisphosphate-dependent interaction of myelin basic protein with the plasma membrane in oligodendroglial cells and its rapid perturbation by elevated calcium. J Neurosci 29:4794–4807. https://doi.org/10.1523/JNEUROSCI.3955-08.2009
8. Aggarwal S, Yurlova L, Snaidero N, Reetz C, Frey S, Zimmermann J, Pähler G, Janshoff A et al (2011) A size barrier limits protein diffusion at the cell surface to generate lipid-rich myelin-membrane sheets. Dev Cell 21:445–456. https://doi.org/10.1016/j.devcel.2011.08.001
9. Pollard TD, Blanchoin L, Mullins RD (2000) Molecular mechanisms controlling actin filament dynamics in nonmuscle cells. Ann Rev Biophys Biomol Struct 29:545–576. https://doi.org/10.1146/annurev.biophys.29.1.545
10. Kim H-J, DiBernardo AB, Sloane JA, Rasband MN, Solomon D, Kosaras B, Kwak SP, Vartanian TK (2006) WAVE1 is required for oligodendrocyte morphogenesis and normal CNS myelination. J. Neurosci 26:5849–5859. https://doi.org/10.1523/JNEUROSCI.4921-05.2006
11. Xue B, Robinson RC (2013) Guardians of the actin monomer. Eur J Cell Biol 92(10-11):316–332. https://doi.org/10.1016/j.ejcb.2013.10.012
12. Guardiola-Diaz HM, Ishii A, Bansal R (2012) Erk1/2 MAPK and mTOR signaling sequentially regulates progression through distinct stages of oligodendrocyte differentiation. Glia 60:476–486
13. Narayanan SP, Flores AI, Wang F, Macklin WB (2009) Akt signals through the mammalian target of rapamycin pathway to regulate CNS myelination. J Neurosci 29:6860–6870
14. Tyler WA, Gangoli N, Gokina P, Kim HA, Covey M, Levison SW, Wood TLJ (2009) Activation of the mammalian target of rapamycin (mTOR) is essential for oligodendrocyte differentiation. Neurosci 29:6367–6378
15. Bercury KK, Dai J, Sachs HH, Ahrendsen JT, Wood TL, Macklin WB (2014) Conditional ablation of raptor or rictor has differential impact on oligodendrocyte differentiation and CNS myelination. J Neurosci 34:4466–4480
16. Fancy SP, Baranzini SE, Zhao C, Yuk DI, Irvine KA, Kaing S, Sanai N, Franklin RJ et al (2009) Dysregulation of the Wnt pathway inhibits timely myelination and remyelination in the mammalian CNS. Genes Dev 23:1571–1585
17. Feigenson K, Reid M, See J, Crenshaw EB 3rd, Grinspan JB (2009) Wnt signaling is sufficient to perturb oligodendrocyte maturation. Mol Cell Neurosci 42:255–265
18. Ye F, Chen Y, Hoang T, Montgomery RL, Zhao XH, Bu H, Hu T, Taketo MM et al (2009) HDAC1 and HDAC2 regulate oligodendrocyte differentiation by disrupting the beta-catenin-TCF interaction. Nat Neurosci 12:829–838

19. Kalani MY, Cheshier SH, Cord BJ, Bababeygy SR, Vogel H, Weissman IL, Palmer TD, Nusse R (2008) Wnt-mediated self-renewal of neural stem/progenitor cells. Proc Natl Acad Sci 105: 16970–16975
20. Ortega F, Gascón S, Masserdotti G, Deshpande A, Simon C, Fischer J, Dimou L, Chichung Lie D et al (2013) Oligodendrogliogenic and neurogenic adult subependymal zone neural stem cells constitute distinct lineages and exhibit differential responsiveness to Wnt signalling. Nat Cell Biol 15:602–613
21. Tawk M, Makoukji J, Belle M, Fonte C, Trousson A, Hawkins T, Li H, Ghandour S et al (2011) Wnt/beta-catenin signaling is an essential and direct driver of myelin gene expression and myelinogenesis. J Neurosci 31:3729–3742
22. Nabi IR, Shankar J, Dennis JW (2015) The galectin lattice at a glance. J Cell Sci 128:2213–2219. https://doi.org/10.1242/jcs.151159
23. Laderach DJ, Compagno D, Toscano MA, Croci DO, Dergan-Dylon S, Salatino M, Rabinovich GA (2010) Dissecting the signal transduction pathways triggered by galectin–glycan interactions in physiological and pathological settings. IUBMB Life 62:1–13. https://doi.org/10.1002/iub.281.
24. Saravanan C, Liu FT, Gipson IK, Panjwani N (2009) Galectin-3 promotes lamellipodia formation in epithelial cells by interacting with complex N-glycans on alpha3beta1 integrin. J Cell Sci 122: 3684–3693. https://doi.org/10.1242/jcs.045674
25. Lagana A, Goetz JG, Cheung P, Raz A, Dennis JW, Nabi IR (2006) Galectin binding to Mgat5-modified N-glycans regulates fibronectin matrix remodeling in tumor cells. Mol Cell Biol 26:3181–3193. https://doi.org/10.1128/MCB.26.8.3181-3193.2006
26. Pasquini LA, Millet V, Hoyos HC, Giannoni JP, Croci DO, Marder M, Liu FT, Rabinovich GA et al (2011) Galectin-3 drives oligodendrocyte differentiation to control myelin integrity and function. Cell Death Differ 18:1746–1756. https://doi.org/10.1038/cdd.2011.40
27. Hoyos HC, Rinaldi M, Mendez-Huergo SP, Marder M, Rabinovich GA, Pasquini JM, Pasquini LA (2014) Galectin-3 controls the response of microglial cells to limit cuprizone-induced demyelination. Neurobiol Dis 62:441–455. https://doi.org/10.1016/j.nbd.2013.10.023
28. Hoyos HC, Marder M, Ulrich R, Gudi V, Stangel M, Rabinovich GA, Pasquini LA, Pasquini JM (2016) The role of galectin-3: from oligodendroglial differentiation and myelination to demyelination and remyelination processes in a cuprizone-induced demyelination model. Adv Exp Med Biol 949:311–332. https://doi.org/10.1007/978-3-319-40764-7_15.
29. Haines JD, Vidaurre OG, Zhang F, Riffo-Campos ÁL, Castillo J, Casanova, Casaccia P, Lopez-Rodas G (2015) Multiple sclerosis patient-derived CSF induces transcriptional changes in proliferating oligodendrocyte progenitors. Mult Scler 21:1655–1669. https://doi.org/10.1177/1352458515573094
30. Salomonsson E, Carlsson MC, Osla V, Hendus-Altenburger R, Kahl-Knutson B, Oberg CT, Sundin A, Nilsson R et al (2010) Mutational tuning of galectin-3 specificity and biological function. J Biol Chem 285:35079–35091. https://doi.org/10.1074/jbc.M109.098160
31. Gonsalvez D, Ferner AH, Peckham H, Murray SS, Xiao J (2016) The roles of extracellular related-kinases 1 and 2 signaling in CNS myelination. Neuropharmacology 110:586–593. https://doi.org/10.1016/j.neuropharm.2015.04.024.
32. Gaesser JM, Fyffe-Maricich SL (2016) Intracellular signaling pathway regulation of myelination and remyelination in the CNS. Exp Neurol 283:501–511. https://doi.org/10.1016/j.expneurol.2016.03.008.
33. Wheeler NA, Fuss B (2016) Extracellular cues influencing oligodendrocyte differentiation and (re)myelination. Exp Neurol 283: 512–530. https://doi.org/10.1016/j.expneurol.2016.03.019
34. Liu Z, Xu D, Wang S, Chen Y, Li Z, Gao X, Jiang L, Tang Y et al (2017) Astrocytes induce proliferation of oligodendrocyte progenitor cells via connexin 47-mediated activation of the ERK/Id4 pathway. Cell Cycle 16:714–722. https://doi.org/10.1080/15384101.2017.1295183
35. Kuroda M, Muramatsu R, Yamashita T (2017) Cardiomyocyte-released factors stimulate oligodendrocyte precursor cells proliferation. Biochem Biophys Res Commun 482:1160–1164. https://doi.org/10.1016/j.bbrc.2016.12.004
36. Alge-Priglinger CS, André S, Schoeffl H, Kampik A, Strauss RW, Kernt M, Gabius HJ, Priglinger SG (2011) Negative regulation of RPE cell attachment by carbohydrate-dependent cell surface binding of galectin-3 and inhibition of the ERKeMAPK pathway. Biochimie 93:477–488. https://doi.org/10.1016/j.biochi.2010.10.021
37. Mendoza MC, Er EE, Zhang W, Ballif BA, Elliott HL, Danuser G, Blenis J (2011) ERK-MAPK drives lamellipodia protrusion by activating the WAVE2 regulatory complex. Mol Cell 41:661–671. https://doi.org/10.1016/j.molcel.2011.02.031
38. Morley SC, Sung J, Sun GP, Martelli MP, Bunnell SC, Bierer BE (2007) Gelsolin overexpression alters actin dynamics and tyrosine phosphorylation of lipid raft-associated proteins in Jurkat T cells. Mol Immunol 44:2469–2480. https://doi.org/10.1016/j.molimm.2006.09.024
39. Buongiorno P, Pethe VV, Charames GS, Esufali S, Bapat B (2008) Rac1 GTPase and the Rac1 exchange factor Tiam1 associate with Wnt-responsive promoters to enhance beta-catenin/TCF-dependent transcription in colorectal cancer cells. Mol Cancer 7:73. https://doi.org/10.1186/1476-4598-7-73
40. Wu X, Tu X, Joeng KS, Hilton MJ, Williams DA, Long F (2008) Rac1 activation controls nuclear localization of b-catenin during canonical Wnt signaling. Cell 133:340–353. https://doi.org/10.1016/j.cell.2008.01.052
41. Thurnherr T, Benninger Y, Wu X, Chrostek A, Krause SM, Nave KA, Franklin RJ, Brakebusch C et al (2006) Cdc42 and Rac1 signaling are both required for and act synergistically in the correct formation of myelin sheaths in the CNS. J Neurosci 26:10110–10119
42. Flores AI, Narayanan SP, Morse EN, Shick HE, Yin X, Kidd G, Avila RL, Kirschner DA et al (2008) Constitutively active Akt induces enhanced myelination in the CNS. J Neurosci 28(28): 7174–7183
43. Goebbels S, Oltrogge JH, Kemper R, Heilmann I, Bormuth I, Wolfer S, Wichert SP, Möbius W et al (2010) Elevated phosphatidylinositol 3,4,5-trisphosphate in glia triggers cell-autonomous membrane wrapping and myelination. J Neurosci 30: 8953–8964. https://doi.org/10.1523/JNEUROSCI.0219-10.2010
44. Harrington EP, Zhao C, Fancy SP, Kaing S, Franklin RJ, Rowitch DH (2010) Oligodendrocyte PTEN is required for myelin and axonal integrity, not remyelination. Ann Neurol 68(5):703–716
45. Figlia G, Gerber D, Suter U (2017) Myelination and mTOR. Glia: 1–15. https://doi.org/10.1002/glia.23273.
46. Hermida MA, Dinesh Kumar J, Leslie NR (2017) GSK3 and its interactions with the PI3K/AKT/mTOR signalling network. Adv Biol Regul 65:5–15. https://doi.org/10.1016/j.jbior.2017.06.003
47. Song S, Mazurek N, Liu C, Sun Y, Ding QQ, Liu K, Hung MC, Bresalier RS (2009) Galectin-3 mediates nuclear beta-catenin accumulation and Wnt signaling in human colon cancer cells by regulation of glycogen synthase kinase-3beta activity. Cancer Res 69(4): 1343–1349
48. Rotty JD, Wu C, Haynes EM, Suarez C, Winkelman JD, Johnson HE, Haugh JM, Kovar DR et al (2014) Profilin-1 serves as a gatekeeper for actin assembly by Arp2/3-dependent and -independent pathways. Dev Cell 32:54–67. https://doi.org/10.1016/j.devcel.2014.10.026

49. Montani L, Buerki-Thurnherr T, de Faria JP, Pereira JA, Dias NG, Fernandes R, Gonçalves AF, Braun A et al (2014) Profilin 1 is required for peripheral nervous system myelination. Development 141:1553–1561. https://doi.org/10.1242/dev.101840.

50. Dai J, Bercury KK, Macklin WB (2014) Interaction of mTOR and Erk1/2 signaling to regulate oligodendrocyte differentiation. Glia 62(12):2096–2109